

Spreading and Vectoring of a Subsonic Axisymmetric Air Jet by Plasma Actuator: a Preliminary Study.

Nicolas BENARD, Jerome JOLIBOIS, Maxime FORTE, Gerard TOUCHARD and Eric MOREAU

*Laboratoire d'études aérodynamiques, Unité Mixte C.N.R.S. 6609,
Bd Marie et Pierre Curie, téléport 2, 86962 Futuroscope Chasseneuil, France.
nicolas.benard@lea.univ-poitiers.fr*

Abstract. Passive and active control devices are usually investigated in order to enhance the external aerodynamic or aeroacoustic characteristics. Non-thermal surface plasma actuators have demonstrated their efficiency for airflow modification over bluff body. This study presents a new application of a subsonic axisymmetric air jet control using a barrier dielectric discharge. This discharge is able to produce a local flow (usually called “electric wind”) close to the dielectric with a large exciting frequency range. A flow naturally attached to the bevel of an axisymmetric jet diffuser is separated by momentum addition in the shear layer. Laser Doppler Velocimetry measurements are performed to fully explore the cross stream velocity profiles. A jet deflection and an enhancement of the turbulent components are observed and partially quantified. Quasi-steady and unsteady actuations are performed and an optimal excitation frequency is pointed out. The time scale of the separation and reattachment process is also introduced and demonstrates that this actuator is suitable for a dynamic control of the flow phenomena occurring in axisymmetric non reactive jets.

Key words: flow control, non-thermal plasma, axisymmetric jet, shear layer, jet mixing.

1. Introduction

Active control techniques finally involve imparting perturbations to the jet shear layer in order to achieve significant jet mixing, spreading or jet vectoring. These are usually performed by appropriate steady or unsteady excitations at strategic locations and plasma actuators appear to be a promising alternative to mechanical and fluidic control devices. The increasing popularity of the non-thermal surface plasma actuators is evidenced by the wide diversity of their applications in flow control [1]. Flow separation and reattachment above airfoils [2-3], control of vortex shedding at cylinder edges [4] or delay of the boundary layer transition [5] can be achieved using surface plasma actuators with promising results. This device should also complete the actual synthetic jet actuators for the manipulation of the shear layer at an axisymmetric air jet by forcing the flow structure. These actuators consist of thin conductive electrodes placed in contact with the flow to be forced. An electrohydrodynamic force is generated by applying an high-voltage between the electrodes. This body forces derive from charged particles (ions) appearing in the inter electrode space and the momentum transfer from the ionized particles to the neutral atmospheric air component produces a local flow usually called “electric wind”. This local velocity flow

usually tangents the dielectric wall supporting the electrodes and allows to manipulate the boundary layer and add momentum in the shear layer [1]. Non-thermal plasma actuators act at the shear layer scale and constitute an active control device without mechanical part therefore avoiding mass addition, sources of noise and vibrations. Contrary to the sometimes heavy, complex or expensive mechanical active devices, a jet mixing enhancement or thrust vectoring by plasma actuators could be transposed to civil or military aircrafts.

The research reported in this paper concerns the first step of the control of an axisymmetric air jet equipped with a small angle (12°) diffuser exit. The flow naturally attached to the diffuser bevel is experimentally separated using a barrier dielectric discharge (DBD) actuator. The global behaviour of the unforced and forced air jet for a jet velocity of $20 \text{ m}\cdot\text{s}^{-1}$ is investigated using Laser Doppler Velocimeter for steady and unsteady actuations. The input signal dependence is explored via the study of the imposed signal waveform. Unsteady actuation is also performed in order to excite the flow instabilities at different Strouhal numbers and various duty-cycle values are investigated.

2. Experimental facility

In this study, the jet diameter upstream the diffuser is 50 mm. The diffuser has a small angle (12° compared to the jet direction), the bevel is 30 mm long and the resulting exit diameter is 62.5 mm (Fig. 1). All the pieces are made of a dielectric material (vinyl polychloride). In this configuration, the air flow is naturally attached to the bevel for jet centerline velocity ranging from 10 to $40 \text{ m}\cdot\text{s}^{-1}$. Measures are performed with a primary jet velocity of $20 \text{ m}\cdot\text{s}^{-1}$ (Reynolds number of 64,100). A circular rough band made of aluminum oxide ($h=350 \mu\text{m}$) is stuck 200 mm upstream the diffuser exit in order to impose the laminar to turbulent transition. The low speed wind tunnel facility is a circular open-air one with a jet exit of 50 mm obtained by mean of a contraction outlet (contraction ratio of 1:17). The air flow is driven by a centrifugal fan (FEVI F18G-1R-500, France) delivering $0.3 \text{ m}^3\cdot\text{s}^{-1}$. A fog generator (Deltalab, EI511) atomizes pharmaceutical oil (Deltalab, Ondina 15) into fine droplets ($d_{\text{droplets}}=0.5\text{-}2 \mu\text{m}$) dedicated to the laser light scattering and the produced smoke is injected into the fan ventilator.

Time-averaged velocity and turbulent components are measured using laser Doppler velocimeter (LDV). The light source is a 5 W Argon-ion laser. Blue and green beams (wavelengths of 514 and 488 nm respectively) composed the measurement volume. The optical system is fixed on a micrometric displacement system ($\pm 0.01 \text{ mm}$). The sampling frequency varies between 10 kHz and 20 kHz and 40.000 bursts are stored for each acquisition point of the velocity profiles. Data are computed with a flow velocity analyser provided by Dantec. For all the LDV measurements, the origin is located at the diffuser exit, at the intersection of the vertical and horizontal symmetry planes (see figure 1).

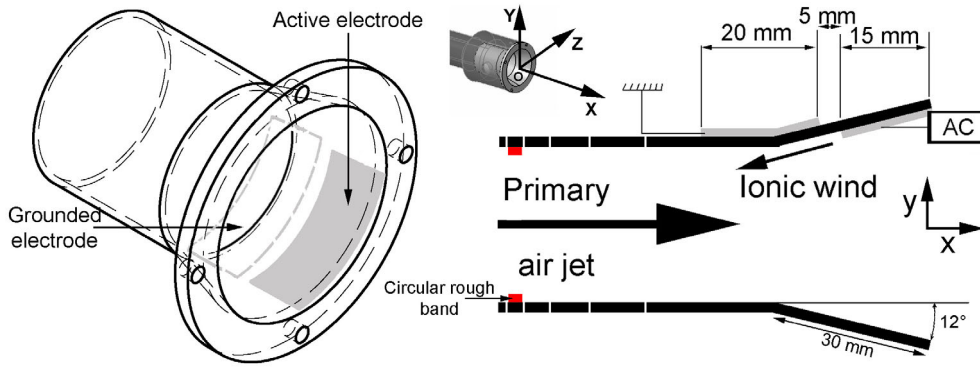


Figure 1: Schematic view of the nozzle geometry and electrodes location.

The lower electrode is grounded and the non-thermal plasma is generated by exciting the active electrode with an AC high-voltage generated by a HV power amplifier TREK 30/20A (20 mA, 20 kHz). The DBD actuators require being supply by an alternative voltage but yet steady or unsteady actuations are often considered [6]. For electric signal period largely lower than the fluid response (approximately 10 ms according to Forte et al. [7]), the velocity created by the actuator is considered as a steady excitation. Unsteady signals are performed by cycling a first AC ‘steady’ signal by a pulse signal of lower frequency (Fig. 2a). By controlling the pulse duration, duty-cycle values (the pulse duration (t) divided by the pulse period (T)) could be adjusted. In this study, the steady actuator mode is defined by a sine $40\text{kV}_{\text{p-p}}$ high-voltage modulated by a 1.5 kHz frequency. For unsteady actuations the signal is triggered by pulse periods corresponding to Strouhal numbers ($St=fd/U_{\infty}$ where $d=50\text{mm}$) ranging between 0.05 and 1.

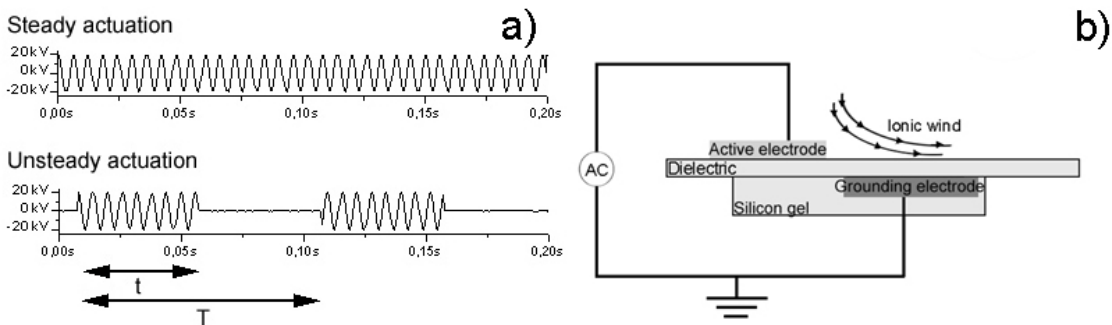


Figure 2. (a): Steady and unsteady actuation modes. (b): DBD actuator principle.

3. The dielectric barrier discharge actuator

The DBD is characterized by a stable and nearly homogeneous discharge over the whole surface. The arc transition is prevented by the dielectric barrier and the

micro discharges are uniformly distributed in time and space from the right edge of the active electrode to the left. In this study, the surface DBD is generated between two thin aluminium electrodes ($e=0.1$ mm) separated by a 3-mm-thick dielectric (vinyl polychloride) (Fig. 2b). The grounded electrode is encapsulated with silicon gel avoiding the production of ionic wind below the dielectric. The discharge only occurs on the upstream side of the top electrode. Details of the retained DBD configuration are available in the figure 1. The active electrode is placed tangentially at the lip of the diffuser and its spanwise length is 40 mm (Fig. 1). The DBD action takes place in approximately $\frac{1}{4}$ of the exit diameter (45°). In this configuration, the produced ionic wind occurs in a counter-flow mode allowing a pressure gradient increase (in the azimuthal direction) and a flow separation along the bevel of the diffuser. Pitot measurements in this electrode configuration have demonstrated (in free stream condition) that a maximal velocity of 6.2 m.s^{-1} is reached at 0.5 mm of the bevel wall for a 40kV_{p-p} high-voltage and a frequency of 1.5kHz [8]. The produced fluid velocity is concentrated in a thin layer of approximately 4 mm. This actuator seems to be particularly efficient for a targeted control of the shear layer because the force created by the control device generally needs to be located near the reattachment or the separation point occurring close to the wall. All the results of this study are obtained with a single DBD actuator located at the upper bevel. Electrical measurements have demonstrated that the mean power consumption for this electrode configuration is 4.8W for a 40kV_{p-p} high-voltage and a frequency of 1.5kHz.

4. Results

4.1 THE DBD EFFECT ON VELOCITY PROFILES

The distribution of the normalized time-averaged and RMS velocity at the exit plane of the primary air jet ($x/D=0.1$) are plotted in figure 3 for the baseline and air jet forced by a ‘steady’ actuation. The baseline profiles present symmetric distribution over the cross stream direction with single peak velocity. As expected, without control, the RMS is symmetric with respect to the centreline and it presents a double peak distribution. The potential core turbulence level is around 3-4% and the velocities in this region are uniform within $\pm 0.007 U_j$. The shape factor (H) of the boundary layer corresponds to a fully turbulent regime partly due to the circular rough ($H=1.15$ with displacement and momentum thickness computed on the distance between the potential core and a jet diameter of 50 mm).

The counter flow induced by the DBD actuator produces a velocity decrease in the upper part of the jet with a partial fluid separation along the upper bevel of the diffuser. The lower part of the forced air jet presents a slight velocity increase

under DBD actuation. The modified airflow exhibits an increase of the velocities fluctuations at the upper part of the diffuser (increase of $\approx 40\%$ in u'). This increase in turbulent intensity is balanced by a small decrease and width reduction at the lower part of the diffuser ($\approx -10\%$ in u'). The turbulent intensity remains constant in the potential core and the effects of the flow control on the RMS levels are larger on the side closer to the control device.

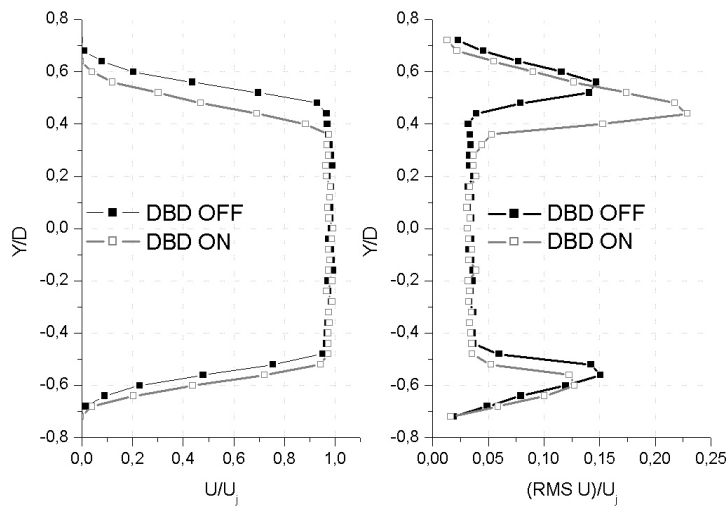


Figure 3: Time-averaged and rms distribution of the primary velocity component ($x/D=0.1$)

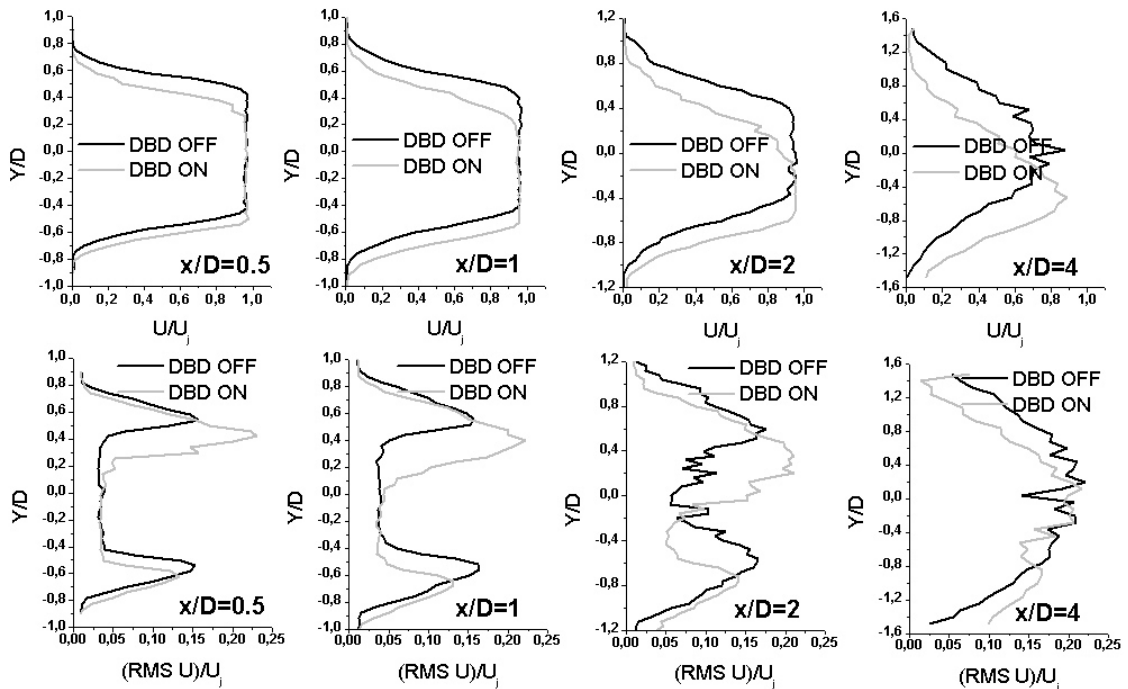


Figure 4: Longitudinal evolution of the time-averaged and rms distribution ($0.5 < x/D < 4$)

The flow separation at the upper bevel induces a deflection of the primary air jet (Fig. 4). The vectoring angle (defined as the angle between the x-direction and the line that follows the maximum velocity) is about 13.5° and is comparable to results obtained by mechanical device or fluidic flow control [9-10]. The turbulent intensity is promoted close to the diffuser ($x/D < 4$) and it seems that the large scale flow structures are transformed into small eddies. The low frequency noise could be manipulated by the actuator and a spectra noise reduction could be predicted. An improvement of the jet mixing could also be expected at the diffuser exit.

4.2 DEPENDENCE TO THE SIGNAL WAVEFORM

Contrary to the ionic velocity directly related to the signal supplied to the electrodes in amplitude and frequency [8], the effects of the signal waveform remain unclear. In this section, the velocity profiles (at $x/D=1$) for a sinusoidal and a triangular AC input waveform are compared for $40\text{kV}_{\text{p-p}}$ at a frequency of 1.5kHz . The results showed in figure 5 demonstrate that this choice of waveform have few consequence neither on the jet deflection nor on the rms distribution and values.

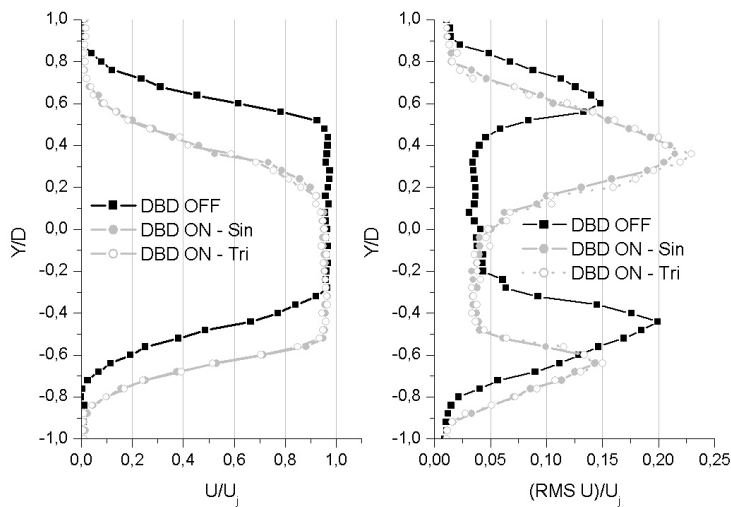


Figure 5: Time-averaged and rms distribution of the primary velocity component for sinusoidal and triangular signal waveforms ($x/D=1$)

In parallel to the LDV measurements, the voltage signal was acquired during the experiment session. The sinusoidal waveform presents large deformation at the peak values due to the low slew rate of the high-voltage amplifier ($350\text{ V}/\mu\text{s}$). Triangular and sinusoidal signal are nearly similar and the resulted velocity profiles are finally not surprising. New signal waveforms need to be considered in order to fully define a possible fluid response depending on the electric signal.

4.3 EFFECTS OF AN UNSTEADY ACTUATION

Flow separation process is generally based on excitation of natural instabilities. A pulsed addition of momentum can act on the large scale coherent structures existing in shear layers and it has been recognized that unsteady manipulation of these structures could enhance the global fluid response, increase the mixing and spreading of air jet and reduce the low frequency noise level. Unsteady actuations at different excitation frequencies ($St=0.05, 0.2, 0.8$ and 1) are successively investigated at $x/D=0.5$ and the resulting velocity profiles are plotted in figure 6.

Observations of the time-averaged results plotted in figure 6 demonstrate that an unsteady excitation at low Strouhal number induces more velocity reduction in the upper part of the air jet than excitations at high frequency. The lower part of the axisymmetric jet presents no frequency dependence. These observations are also suitable for the turbulent velocity component since the higher part of the jet is wider and more intense for weak Strouhal numbers. An unsteady actuation at low frequency produces more turbulent intensity and consequently is favourable for a mixing enhancement.

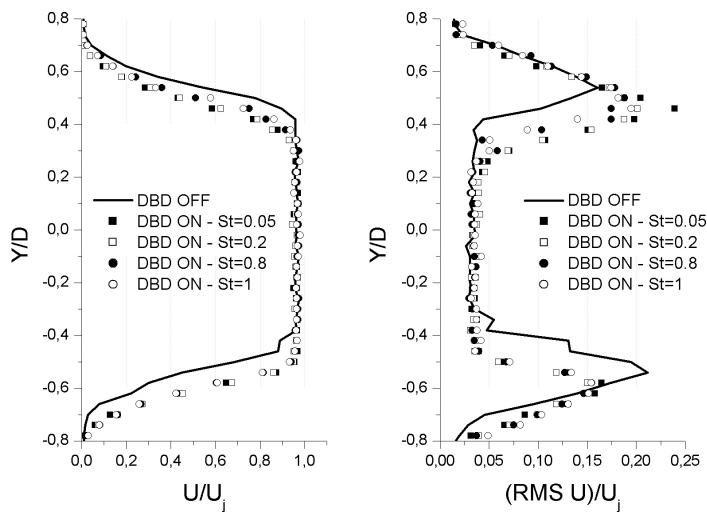


Figure 6: Time-averaged and rms distribution of the velocity for unsteady actuation ($x/D=0.5$)

Strouhal number equal to unity is often considered as a reference to obtain a maximal response effect [6]. In our experimental conditions, a Strouhal number equal to unity corresponds to a 400Hz excitation frequency corresponding to a succession of discharge On during 1.25 ms, follow by a state of discharge Off during 1.25 ms. The non-thermal discharge and induced air velocity is effective 10 ms after the actuation (at $20kV_{p-p}$ and 700Hz) [7], the excitation period is too short to generate a maximal momentum addition in the shear layer and the flow control effects are consequently limited.

An unsteady actuation at a Strouhal number of 0.05 presents a maximum jet deflection compared to others excitation frequencies but this unsteady actuation is not more efficient in jet deflection and mixing enhancement than a quasi-steady one (Fig. 7). This result demonstrates that a Strouhal value of 0.05 do not correspond to the optimal excitation frequency. Future investigations should be focus in an excitation around the natural frequency of the primary mode of the air jet. More, the unsteady actuation should be synchronized with the natural frequencies of the air jet. This should be an objective in the future for a reactive control.

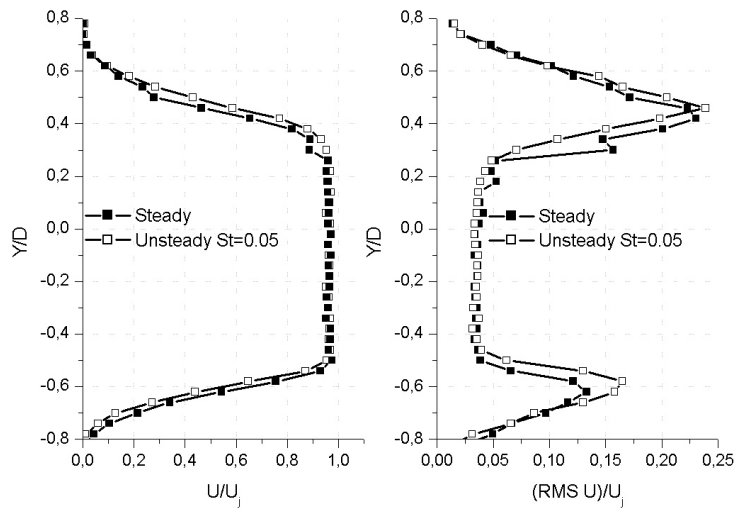


Figure 7: Comparison of time-averaged and rms velocities for steady and unsteady actuation ($x/D=0.5$)

4.4 DUTY-CYCLE ACTUATION

Duty-cycle signals are modulated to investigate a potential electric consumption reduction while preserving a constant overall control effect. Duty-cycle ranging between 50 and 100% of a primary signal sets to $40V_{p-p}$ and 1.5kHz frequency are studied for an air jet forced at 10 and 100Hz ($St=0.025$ and 0.25 respectively) (Fig. 8). The obtained results reveal that a duty-cycle of 80% allows to reach this objective with time-averaged and rms velocities equivalent to a full cycle forcing. The frequency of the duty-cycle has no impact on the optimal duty-cycle regime. Jet deflection and turbulent energy for 80% duty-cycle are similar to those obtained with a steady actuation but the gain in power supplied to the electrodes is significant with a minimizing consumption of 20% (electric consumption reduction of approximately 1W).

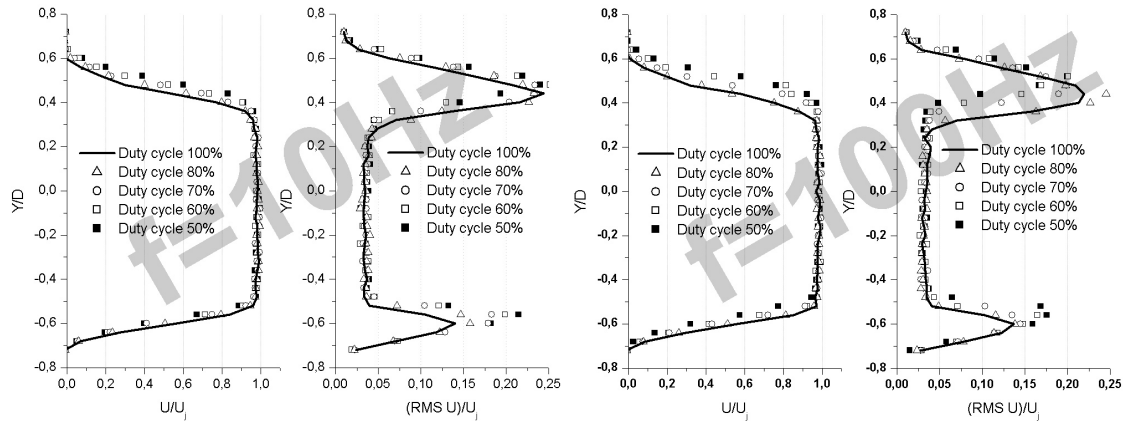


Figure 8: Mean and rms velocities for Duty-cycle at 10 and 100 Hz ($x/D=0.5$)

5. Concluding remarks

In this preliminary study, the macroscopic effects of a DBD actuator on a potential mixing enhancement and jet vectoring are investigated for a subsonic axisymmetric air jet. The control device is implanted on a small-angle diffuser and the airflow produced by the actuator is used to separate a naturally attached flow. Under quasi-steady actuation, results demonstrate that a jet vectoring similar to those obtained with others control devices is conceivable without the drawbacks of mechanical thrust vectoring systems. A quantification of the mixing enhancement properties needs to be performed but these first results report that a reduction of gas noise and temperature could potentially be achieved using non-thermal plasma with an improvement of the stealth characteristics. A parametric study was performed on the supplied high-voltage signal. Whatever the signal imposed is, the control effects are positive and involve a jet vectoring and mixing. Several conclusions could be deduced from the parametric study:

- The input signal waveform could modify the momentum quantity imparted in the shear layer but the investigated sine and triangular waveforms are too similar to induce a clear variation in the global control effect.
- Unsteady actuation at a Strouhal number of 0.05 leads to a better jet deflection compared to others excitation frequencies but unsteady actuation at this frequency has not yet prove to be more efficient than a quasi-steady one.
- Use of a duty-cycle regime could reduce the power consumption of 20% while the forced jet properties are conserved.

Acknowledgements

The authors wish to thank AIRBUS for its financial and technical support (contract #D05028043), under the scientific direction of Dr Stephen Rolston, and J.P. Bonnet, J. Delville and P. Braud (LEA-CEAT, Poitiers) for help us in designing the diffuser geometry and for their advices.

References

1. Moreau, E., Airflow control by non-thermal plasma actuators. *J Phys D: Appl Phys* **40** (2007) 605-636.
2. Sosa, R., Artana, G., Moreau, E. and Touchard G., Stall control at high angle of attack with plasma sheet actuators. *Exps. in Fluids* **42** (2007) 143-167.
3. Corke, T.C., Mertz, B. and Patel, M., Plasma flow control optimized airfoil. *AIAA paper* 2006-1208.
4. McLaughlin, T.E., Felker, B. and Avery, J.C., Further experiments in cylinder wake modification with dielectric barrier discharge forcing. *AIAA paper* 2006-1409.
5. Grundmann, S. and Tropea C., Experimental transition delay using glow-discharge plasma actuators. *Exps in Fluids* (online first).
6. Post, M.L. and Corke T.C., Separation control using plasma actuators – stationary & oscillating airfoils. *AIAA paper* 2004-0841.
7. Forte, M., Leger, L., Pons, J., Moreau, E. and Touchard, G., Plasma actuators for airflow control: measurement of the non-stationary induced flow velocity. *J of Electrostatics* **63** (2005) 929-936.
8. Benard, N., Pons, J., Jolibois, J., Forte, M., Touchard, G. and Moreau E., Airflow control by non thermal plasma actuator: application to control of separation of an air jet naturally attached along the bevel of an axisymmetric diffuser. Proceeding of the 42ème Colloque d'aérodynamique appliquée AAAF, 19-21 April 2007, Nice, France.
9. Bettridge, M.W., Smith, B.L and Spall R.E., Aerodynamic jet steering using steady blowing and suction. *Exps. In Fluids* **40** (2006) 776-785.
10. Ben Chiekh, M., Bera J.C. and Sunyach M., Synthetic jet control for flows in a diffuser: vectoring, spreading and mixing enhancement. *J. of Turbulence* **4** (2003) 1-12.